NIST GCR 99-777

RAPID SCANNING INFRARED/NEAR INFRARED SPECTROMETER: PHASE 2. SBIR. FINAL REPORT

Yudaya Sivathanu, Rony Joseph,
Jongmook Lim, Yuan Zheng and
Jay Gore

United States Department of Commerce
Technology Administration
National Institute of Standards and Technology

NIST GCR 99-777

RAPID SCANNING INFRARED/NEAR INFRARED SPECTROMETER: PHASE 2. SBIR. FINAL REPORT

Prepared for
U.S. Department of Commerce
Building and Fire Research Laboratory
National Institute of Standards and Technology
Gaithersburg, MD 20899

By
Yudaya Sivathanu, Rony Joseph and Jongmook Lim
En'Urga Inc.
1291-A, Cumberland Avenue
West Lafayette, IN 47906
and
Yuan Zheng and Jay Gore
School of Mechanical Engineering
Purdue University
West Lafayette, IN 47907-1003

July 1999
Issued September 1999

Notice

This report was prepared for the Building and Fire Research Laboratory of the National Institute of Standards and Technology under Contract number 50-DKNB-7-90147. The statement and conclusions contained in this report are those of the authors and do not necessarily reflect the views of the National Institute of Standards and Technology or the Building and Fire Research Laboratory.

Table of Contents

Phase II SBIR-Final Report

Rapid Scanning Infrared/Near Infrared Spectrometer

En'Urga Inc.
1291-A, Cumberland Avenue
West Lafayette, IN 47906

prepared for

U.S. Department of Commerce
Building and Fire Research Laboratory
National Institute of Standards and Technology
Gaithersburg, MD 20899

Phase II SBIR: 50-DKNB-7-90147

July, 1999

En'Urga Inc.

ANALYSIS OF COMBUSTION SYSTEMS

Rapid Scanning Infrared/Near Infrared Spectrometer

Yudaya Sivathanu, Rony Joseph and Jongmook Lim
En'Urga Inc.
1291-A, Cumberland Avenue
West Lafayette, IN 47906

and

Yuan Zheng and Jay Gore
School of Mechanical Engineering
Purdue University
West Lafayette, IN 47907-1003

Phase II SBIR: 50-DKNB-7-90147

July, 1999

EXECUTIVE SUMMARY

This Phase II SBIR project report covers the development of a 2-D imaging spectrometer for the determination of the local gas species concentrations and temperatures from a laminar flame, and its extension for commercial application as a gas temperature sensor.

Three separate tasks were undertaken during the Phase II work. The first task was the development of an optimized algorithm and hardware design to obtain gas temperatures from a high frequency multi-wavelength sensor. The second task was the development of an imaging spectrometer to obtain spectral radiation intensities along a horizontal plane from a laminar diffusion flame. The third task was the development of a deconvolution algorithm to obtain gas species concentrations and temperatures from the spectral radiation intensity measurements.

Based on the Phase II research, the following results were obtained. A robust algorithm for determining the gas temperatures at the inlet of a natural gas turbine engine, from measurements of infrared radiation intensities, was developed, evaluated and licensed for commercial production. A study of the different methods of obtaining infrared radiation intensities for a turbine-inlet gas temperature sensor was completed. A prototype 2-D infrared imaging spectrometer was designed, fabricated and delivered to the National Institute of Standards and Technology.

A deconvolution algorithm to obtain local radiation intensities from path integrated measurements was developed and evaluated. The 2-D imaging spectrometer was used to obtain spectrally and spatially resolved infrared radiation intensities in a laminar natural gas diffusion flame. The deconvolution algorithm was used to obtain the local intensities in the laminar natural gas diffusion flame. Reasonable estimates of temperatures were obtained from the local intensities. The estimates of gas concentrations were less satisfactory. The major reason for this behavior is the lack of reliable wavelength calibration. Steps to remedy this are in progress.

A new company called Spectraline Inc. has been started to market the 2-D imaging spectrometer developed during the Phase II research.

Rapid Scanning Infrared/Near Infrared Spectrometer

1. Introduction

Obtaining information on the instantaneous structure of turbulent and transient flames is important in a wide variety of applications such as fire safety, pollution reduction, flame spread studies, and model validation. The different methods for obtaining structure information in reacting flow have been recently reviewed by Durao et al. (1992). These include Tunable Diode Laser Absorption Spectroscopy (TDLAS) (Hanson et al., 1980), Laser Induced Fluorescence (LIF) (Crosley and Smith, 1983) Coherent Anti-Raman Spectroscopy (CARS) (Eckbreth et al., 1979) and Fourier Transform Infrared Spectroscopy (FTIR) (Best et al., 1991), Multi-Wavelength Emission Spectroscopy (MWES) (Sivathanu and Gore, 1991) to mention a few.

LIF and CARS can be used to measure temperatures and species concentrations with much higher spatial resolution than either absorption or emission spectroscopy (Durao et al., 1992). However, the accuracy of these two techniques in the presence of interference is an unknown factor. These techniques have been applied to measurements in laboratory scale turbulent flames (which have no interfering background radiation) with limited success to answer the basic questions on signal strength and accuracy. However, their performance in the presence of interference from particulate contaminants or environmental radiation is unknown. In addition, they require expensive lasers, detectors and signal processing equipment. Therefore, their development into sensors for practical application is not warranted at the present time.

FTIR and MWES are ideal for measuring temperatures, major gas species concentrations and soot volume fractions in turbulent and laminar flames. FTIR and MWES are based on either absorption or emission spectroscopy. Both absorption and emission spectroscopy, in the absence of intrusive probes, measure properties along a path instead of a single point. Therefore, they have to be used in conjunction with deconvolution algorithms to obtain spatially resolved information. FTIR and MWES are however mature technologies and are ideal for exploitation in practical applications unlike laser based techniques such as LIF or TDLAS. Recent development in statistical deconvolution techniques (Vardi and Lee, 1993) have renewed interest in both FTIR and MWES for measuring gas species concentrations, temperatures and soot volume fractions in a wide variety of fires.

Most flames emit significant radiation signatures that are currently used in various applications such as fire detection (Sivathanu and Tseng, 1996), light-off detection (Vaidya et al., 1982), flame diagnostics (Choi et al., 1995), etc. Radiation signatures can be utilized to maximum advantage for determining structural information in turbulent flows (Sivathanu and Faeth, 1990, Sivathanu and Gore, 1991, Sivathanu et al., 1991). Emission spectroscopy does not require a light source, and alignment and data collection are relatively straightforward. Emission spectroscopy is most advantageous in the infrared regions of the spectra, principally because these emission lines arise from transitions in the fundamental bands of stable species such as CO_2 and H_2O. NIR and visible emission typically arise from transitions in the overtones (forbidden transitions) in addition to being from minor species that are not in thermodynamic equilibrium with the flow. Emission spectroscopy also currently offers the most accurate method of temperature determination (Zhu et al., 1997).

Of the various techniques, infrared emission spectroscopy is the most versatile and useful method for obtaining temperature and major gas species concentration information in flames. However, infrared emission spectroscopy is a line of sight method and therefore deconvolution of the line of sight measurements has to be addressed.

Deconvolution of local properties from line of sight measurements is important in a number of applications such as x-ray tomography, nuclear magnetic resonance imaging, atmospheric sciences, optical interferometry and flow field diagnostics. The Radon transform and its analytical solution provide the fundamental framework for a large class of deconvolution problems and their applications as reviewed by Deans (1983). Deconvolution of path integrated measurements requires the inverse Radon transforms. These are usually obtained by fast Fourier transform (Shepp and Logan, 1974), convolution back projection (Ramachandran and Lakshminarayan, 1970), or series expansion methods (Ravichandran and Gouldin, 1988).

In combusting flows, tomography has been used both with absorption (Chen and Goulard, 1976; Santoro et al., 1981), emission (Tourin, 1983, Uchimaya et al., 1985) and simultaneous absorption/emission (Best et al., 1991) spectroscopy to retrieve local properties in axisymmetric and non-axisymmetric laminar flows. Best et al. (1991) used FTIR emission/absorption spectroscopy to obtain qualitative information on soot, species concentrations and temperature in a laminar ethylene/air diffusion flame. Solomon et al. (1986) also used FTIR emission/absorption to obtain soot concentrations, temperatures and radiance due to the gas species in a laminar ethylene/air diffusion flame.

One of the most exciting developments in tomography is the advent of statistical deconvolution algorithms. It has been recently shown (Vardi and Lee, 1993) for systems with strict positivity constraints (i.e. absorption and emission are always greater than one and never negative), that a maximum likelihood approach based on conditional expectations provides convergent solutions. This is a very robust method and was presented before the Royal Statistical Society in 1993. Strict convergence can be proved for a wide array of physical systems ranging from image deblurring to optimal investments (Vardi and Lee, 1993). This statistical deconvolution algorithm based on maximum likelihood estimation has been used for image reconstruction (Shepp and Vardi, 1982, optimizing investment portfolios (Cover, 1984), statistical estimation of censored and grouped data (Bishop et al., 1975), etc.

Intrusive MWES has been used to obtain transient soot volume fractions and temperatures in pool fires (Sivathanu and Faeth, 1990; Sivathanu et al., 1991), and CO_2 concentrations in jet flames. (Sivathanu and Gore, 1991). The disadvantages of the intrusive probes are that they disturb the flow to some unknown degree and it may not be possible to use them in all applications.

To overcome these disadvantages, a discrete probability function (DPF) method was developed to deconvolute path integrated measurements of the Probability Density Functions (PDF) of transmittance in order to obtain the local PDFs of soot concentrations in turbulent flames (Sivathanu and Gore, 1993). Subsequently, statistical deconvolution was used for the simultaneous non-intrusive measurement of soot volume fraction and temperature PDFs in turbulent flames (Sivathanu et al., 1995) using emission tomography. The iterative algorithm is similar to the one proposed by Vardi and Lee (1993) and is based on maximum likelihood estimation. Tomographic methods have also been used for the retrieval of the moments of local transmittances from path integrated measurements (Nyden et al., 1996). During the

Phase I research, retrieval of gas concentrations and temperatures were shown to be feasible (Zhu et al., 1997) using emission spectroscopy in conjunction with RADCAL (Grosshandler, 1980).

Based on the literature review and the Phase I work, emission spectroscopy followed by deconvolution was shown to be one of the more promising techniques for obtaining structure information in laminar, transient, and turbulent flames.

2. Phase II Objectives

There were three objective for the Phase II research work. The first objective was to develop an optimized algorithm to retrieve temperatures at high frequencies from MWES. The second objective was to optimize sensor designs for obtaining infrared emission spectra at high frequencies. The last objective was to develop a 2-D imaging spectrometer to obtain full flow field gas species concentration and temperature information in a laminar flame.

3. Phase II Tasks

Three separate tasks were proposed to accomplish the objectives of the Phase II SBIR. The first task was the development of an optimal algorithm to determine temperatures from measured infrared spectral radiation intensities at several different wavelengths. The second task was the evaluation of different hardware configurations for measuring the spectral radiation intensities at high frequencies. The final task was the development and evaluation of a prototype two-dimensional infrared array for estimation of planar gas concentration and temperatures in laminar flames.

3.1 Algorithm Optimization

The information contained below is proprietary.

****

The temperatures obtained from line of sight measurements in turbulent flames are Planck function weighted temperatures of the non-homogeneous path. The Planck function weighted temperatures are ideal for monitoring combustion instability and pollutant formation. This optimal method of obtaining the Planck function weighted temperatures at high frequencies is to utilize spectral radiation intensity measurements at four wavelengths. Feasibility and algorithm optimization was achieved using two spectral radiation intensity measurements centered around the H_2O band (2470 nm and 2558 nm) and two centered around the CO_2 band (2690 nm and 2870 nm). The 4400 nm CO_2 band is more prominent than the 2780 nm band. However, using the 2700 nm CO_2 band has two advantages; (1) PbS (rather than PbSe) detectors can be used resulting in a very high detector sensitivity, and (2) a silicon (rather than a chalcogenide) optical fiber can be used for remotely monitoring flame radiation. Silicon fibers are less sensitive to degradation and are capable of withstanding higher operating temperatures. These two advantages were sufficient to warrant utilizing the 2700 nm CO_2 band for estimating gas temperatures.

For most commercial applications, the algorithm should be capable of obtaining gas temperatures within 10 ms. Iterative algorithms which use a narrow gas band model are too slow for most commercial applications. Therefore, a temperature look-up-table (LUT), consisting of the intensities at the four wavelengths was developed as part of the first task. To develop the LUT, RADCAL was used to obtain a series of radiation intensities at the four wavelengths by changing the CO_2 and H_2O concentrations as well as temperature. For a path length of 50 mm (typical of those existing in combustors), CO_2 concentrations were varied systematically from 0.050 to 0.07 mole fraction, H_2O concentrations were varied from 0.01 to 0.15 mole fraction and temperatures were varied from 900 to 1500 K. These are the typical ranges present in the overfire region or the exhaust stream of hydrocarbon flames. A total of 65536 intensity sets (intensity at four wavelengths) were obtained by using 32 different CO_2 and H_2O concentrations and 64 temperature values between 900 and 1600 K. The intensities obtained were sorted into an ascending four dimensional table. For implementation, the table is loaded into the computer memory. The measured radiation intensities are converted into temperatures by interpolating within the four dimensional LUT.

To evaluate the LUT, RADCAL (Grosshandler, 1980) was used in a stochastic simulation to obtain random values of spectral radiation intensity at four selected wavelengths. These intensities were calculated using random realizations of temperature, CO_2 and H_2O concentrations. The intensity sets were then used as sensor inputs, and the temperature calculated by interpolation within the four dimensional LUT.

The correlation between the input and the output temperature from the simulations was 0.91. The instantaneous path temperatures and the estimates obtained from the LUT are shown in Fig. 1. Though the mean temperatures were within 5 K, and the correlation was very

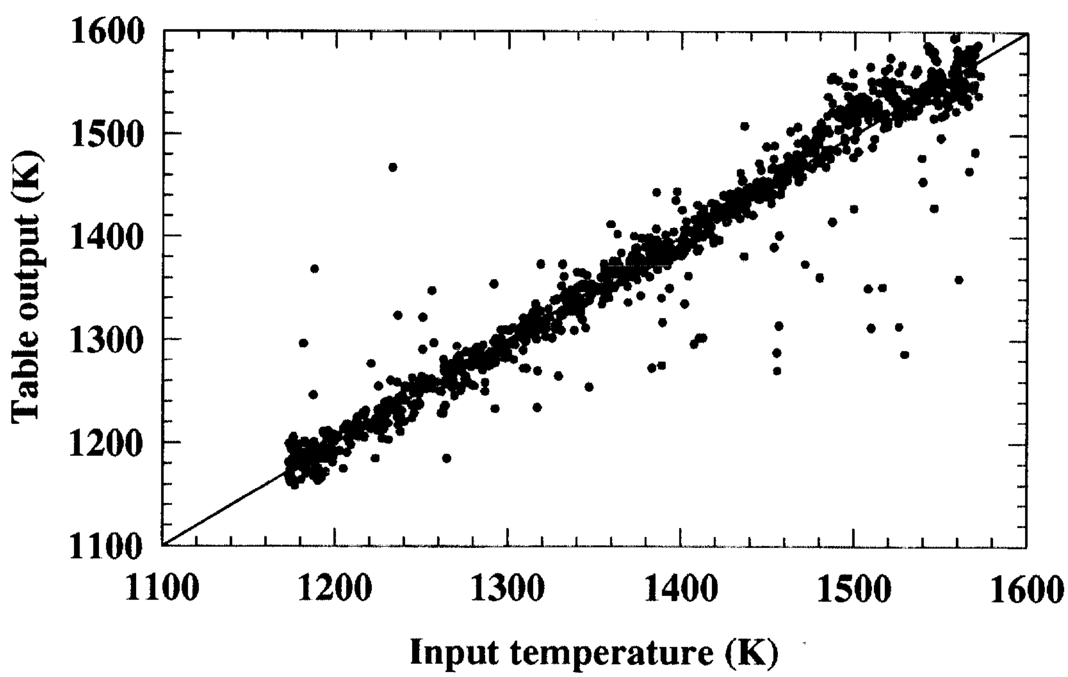

Figure 1. Instantaneous path temperatures and those obtained using the LUT.

high, it is evident that there are many realizations where differences between the true and estimated temperature values were too high. The large differences are obtained when the intensity at any one of the four wavelengths approaches the edge of the values present in the LUT. The best method of reducing this inaccuracy is to use a more finely resolved LUT. However, to minimize the memory requirement of the program, it is more convenient to use two separate LUTs, one for the higher temperature range (1300 to 1600 K) and the other for the lower temperature range (900 to 1300 K).

A new algorithm, which alternates between these two LUTs was implemented. The instantaneous path temperatures and the estimates obtained with the LUTs using the new scheme are shown in Fig. 2. The correlation between the two values increased to 0.96 and the number of points with higher than 100 K error is reduced to a negligible number. In addition, the mean and the RMS temperatures estimated using the LUT are within 1% of the instantaneous path temperatures. The temperatures were obtained within 6 ms using a standard 486 PC. This is sufficiently fast and accurate for most commercial applications. Therefore, the algorithm development proposed in the Phase II research has been successfully completed.

Further refinements in the algorithm will depend on the specific application for which it is used. The methodology to obtain temperature and gas species concentrations from multiple wavelength, infrared radiation intensity measurements at high frequencies has been demonstrated. For different commercial applications En'Urga Inc. will custom design the algorithm. The first commercial application being developed is the determination of gas temperatures at the inlet of a lean premixed natural gas turbine engine.

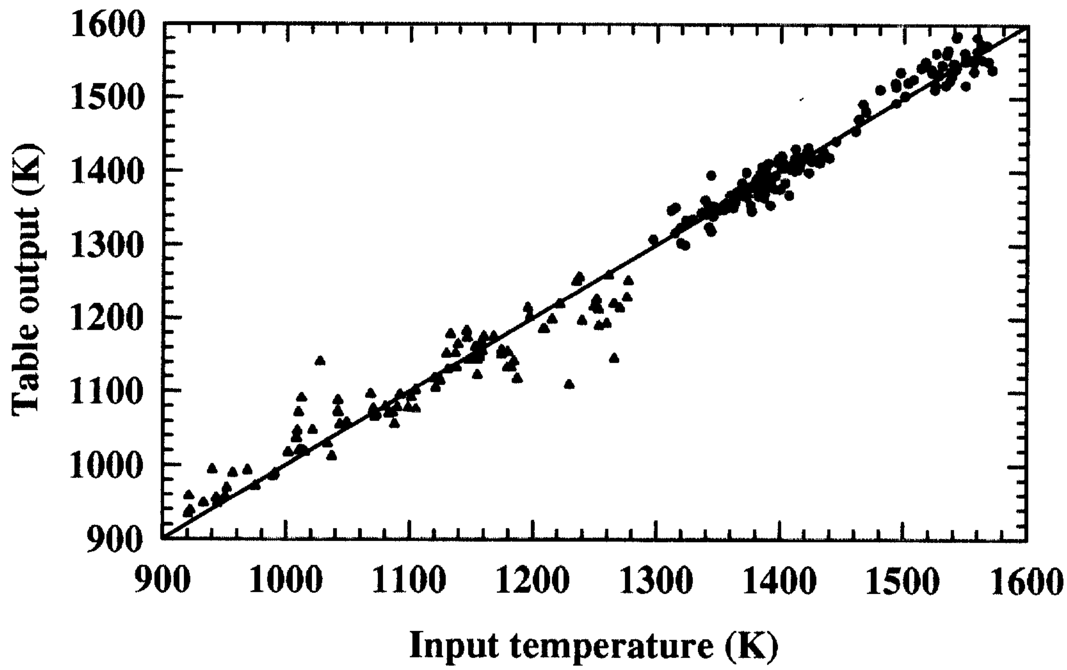

Figure 2. Temperatures estimated using a dual LUT.

En'Urga Inc. has entered into an agreement with AMETEK Power and Industrial Products Inc. to market a multi-wavelength emission sensor for monitoring the gas temperatures at the inlet of a natural gas turbine engine. The prototype development of the sensor has been completed and the sensor was introduced to market during the Joint ASME/IGT conference in June, 1999. Commercial sales is expected to begin during the last quarter of 1999.

****

End of proprietary information

3.2 <u>Hardware Optimization</u>

The second task proposed in the Phase II research was the optimization of the hardware to obtain spectral radiation intensities at several different wavelengths simultaneously. From the algorithm optimization study, it has been demonstrated that obtaining infrared spectral radiation intensities at four wavelengths simultaneously is sufficient for estimating gas temperatures. However for applications that require soot concentrations or CO_2 and H_2O concentrations, the spectral radiation intensities have to be measured at more that four wavelengths.

Any commercial sensor or instrument, that measures spectral radiation intensities simultaneously at several different wavelengths, requires the following elements. (1) A collimating element for restricting the viewing angle of the sensor, (2) a dispersive element to separate the radiation into the different spectral components, and (3) a detecting element to measure the spectral radiation intensities. Table I-III provides the advantages and disadvantages associated with the different types of collimating, dispersing and detecting elements.

Table I: Comparison between different collimating elements

Element	Advantages	Disadvantages
Elongated tube/slit	Simple in design and construction Very precise spatial resolution possible Very tight collimation	Very low radiation throughput Large area detector required to provide spectral separation
Imaging lenses and reflectors	Very high optical throughput Much higher spatial resolution possible Can be used with linear arrays which have very small detecting elements	Design requires correction for chromatic aberration Very tight collimation requires slits in addition to the lenses

The particular choice of collimating, dispersing and detecting element will depend on the application. For a four-wavelength gas temperature sensor, the optimal choice is to use a quadrant detector with a defocusing lens. The different wavelengths are obtained by using optical filters in front of each one of the quadrant detectors. For a research based FTIR or emission spectroscopic instrument, the best possible choice is to utilize a linear array with a prism as the dispersive element. To achieve sufficient optical throughput and also for achieving very good spectral resolution, lenses or reflective components have to be used for the collimating element. The above two configurations are currently being implemented by En'Urga Inc. for an linear imaging spectrometer. The spectrometers are being marketed under the brand name Spectraline. The plastics industry is the first market targeted for the application of the imaging spectrometers.

Table II: Comparison between different dispersing elements

Element	Advantages	Disadvantages
Filter wheel	Simple in design Very precise wavelength separation Maximum light throughput Single element detector can be used	Frequency limited by filter wheel (30 Hz) Moving elements subject to wear and tear Construction is complicated Limited from four to six wavelengths
Dispersion grating	No moving parts Can be used to measure a large number of wavelengths High spectral resolution	Requires order sorting filter Complicated design to achieve correct wavelength identification Very low radiation throughput Requires multiple element detectors
Prism	No moving parts Can be used to measure a large number of wavelengths Relatively high optical throughput	Very tight tolerances required in their design and construction Requires multiple element detectors

Table III: Comparison between different detecting elements

Element	Advantages	Disadvantages
Single element detector	Very inexpensive A variety of detector materials available High sensitivity possible	Can be used only with the filter wheel Very low frequencies
Quadrant detectors	Can be used with imaging lenses Wide variety of detector materials Optical filters can be used instead of dispersing elements	Design requires defocusing lens Limited to four wavelengths
Linear array	Very high frequencies possible Large number of wavelengths High spectral resolution	Very expensive Limited number of detector materials Very involved optical design

3.3. Hardware Development of the 2-D Imaging Spectrometer

The final task of the proposed Phase II SBIR work is to design, calibrate and evaluate a 2-D imaging spectrometer for obtaining planar gas species concentrations and temperatures in a laminar flame. A 320 x 244 element PtSi array camera (PRISM-DS) was purchased from FLIR Systems Inc. The array is in a Stirling cooled package and is used by different industries for obtaining surface temperatures. The first task performed by En'Urga Inc. was to remove the wavelength limiting filter (3000 to 5000 nm) that was present in front of the PRISM-DS camera. In addition, the manufacturer uses a combination of hardware and software to obtain temperatures. These were modified so as to obtain raw pixel voltages, which after calibration with a blackbody can be converted to radiation intensities. An ITI frame grabber board with 12-bit image resolution was purchased to acquire and store the raw pixel voltages.

It was initially proposed to add a moving etalon in front of the camera to obtain the required wavelength dispersion. It was also proposed to obtain a 2-D image, one wavelength at a time. This restricts the system to laminar flames, since most frame grabbers are restricted to 30 Hz. After an extensive market survey, it has been determined that it is more advantageous to obtain a linear image with simultaneous acquisition of the spectral radiation intensities at multiple wavelengths. For a full flow field infrared image, linear scans (one line at a time) can be performed as planned in the Phase II proposal.. Therefore, it was decided to modify the front end of the camera so as to obtain wavelengths along one axis of the 2-D array and a linear dimension along the other axis.

The proposed optical design of the 2-D imaging spectrometer is shown in Fig. 3. The imaging spectrograph system comprises of two independent optical sub systems, a telescope

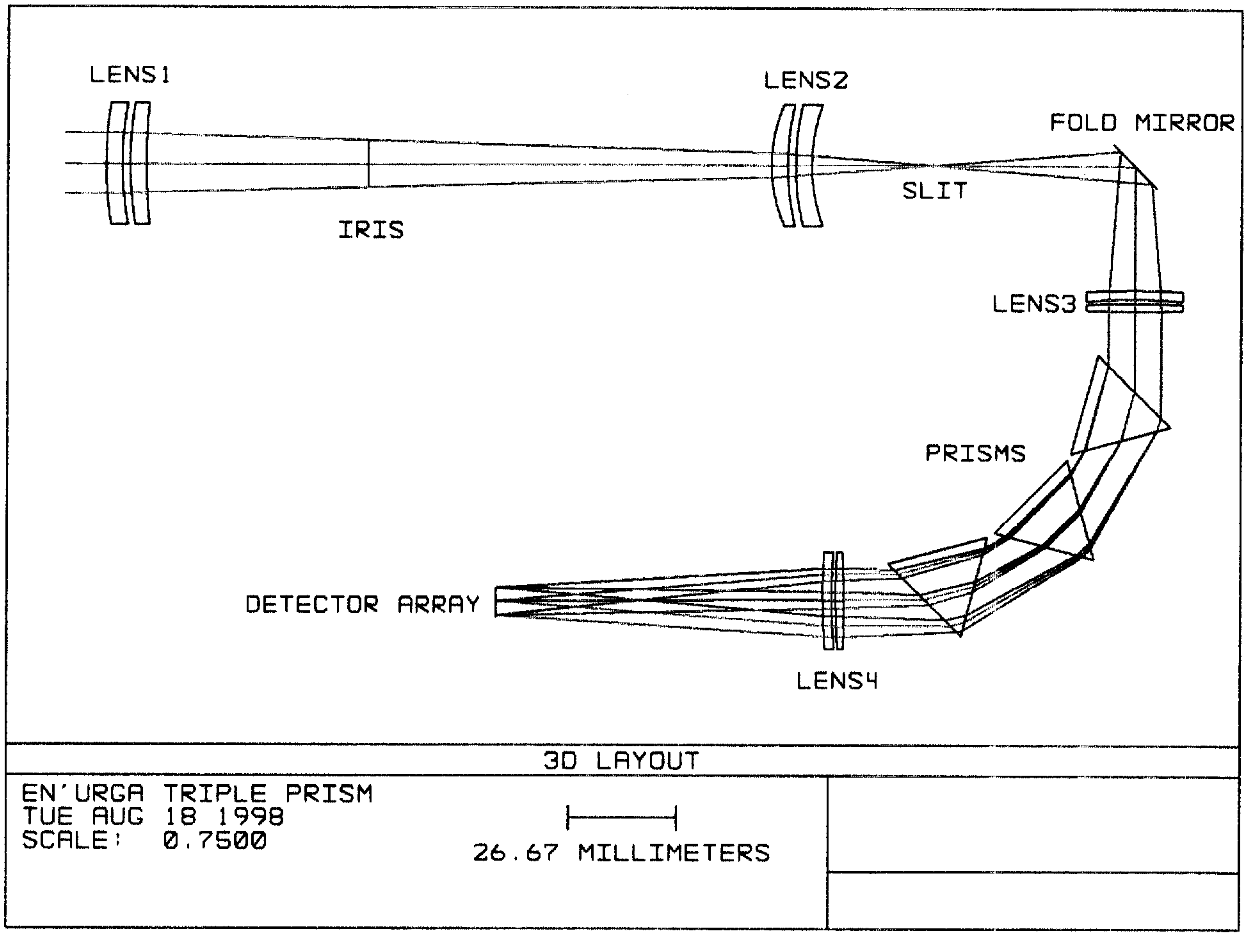

Figure 3. Design of the optical front end of the 2-D imaging spectrometer.

and a prism spectrograph. The telescope is constructed from two lens assemblies, lens1 and lens2. Each lens assembly is an air-spaced silicon/germanium achromatic doublet. The lenses are optimized for diffraction limited performance from 2.5 to 4.75 microns. The effective focal length of the telescope is 128 mm. A 50 mm object located 500 mm in front of the first lens results in a 9.6 mm image located 30 mm after the last lens. A slit is placed at this intermediate image. An aperture stop is located between the lens assemblies. The resulting exit pupil of the telescope is located 242 mm after the image, matching the entrance pupil of the prism spectrograph.

The prism spectrograph begins with the slit image of the telescope. Two identical air-spaced silicon/germanium achromatic doublets (Lens3 and Lens4) form a 1:1 image of the slit onto the long axis of a 9.6 x 7.32 mm detector array. Three 1" equilateral CaF2 prisms are placed in collimated space to provide the dispersion necessary to spread the 2.5 to 4.75 micron spectrum across the 7.32 mm short axis of the detector array. This arrangement yields an f/6 beam in image space. The diffraction limited point spread function diameters range from 36 to 70 um across the 2.5 to 4.75 micron spectral range.

The detector array consists of 30 um square pixels. A series of tradeoff studies lead to the selection of this optical system. It was determined that the system needed to be f/6 or less in image space. Higher f-numbers resulted in diffraction limited spot sizes that significantly exceeded the dimensions of the detector pixels. To achieve f/6 performance, either a very large (>2") prism or a series of smaller prisms was required. Several single-pass and Litrow prism configurations were examined. A system of three 1" prisms in single-pass was selected due to the significant expense of having larger prisms manufactured. The length of the prism chain requires a pupil (image of the iris) to be placed in the middle prism to avoid vignetting. The location of this pupil and size of the entrance slit set the specifications of the telescope system. Three separate telescope designs were considered, and a straightforward two-lens system was chosen as a compromise between system length and optical design complexity.

A schematic layout of the final assembly as completed is shown in Figure 4. The light

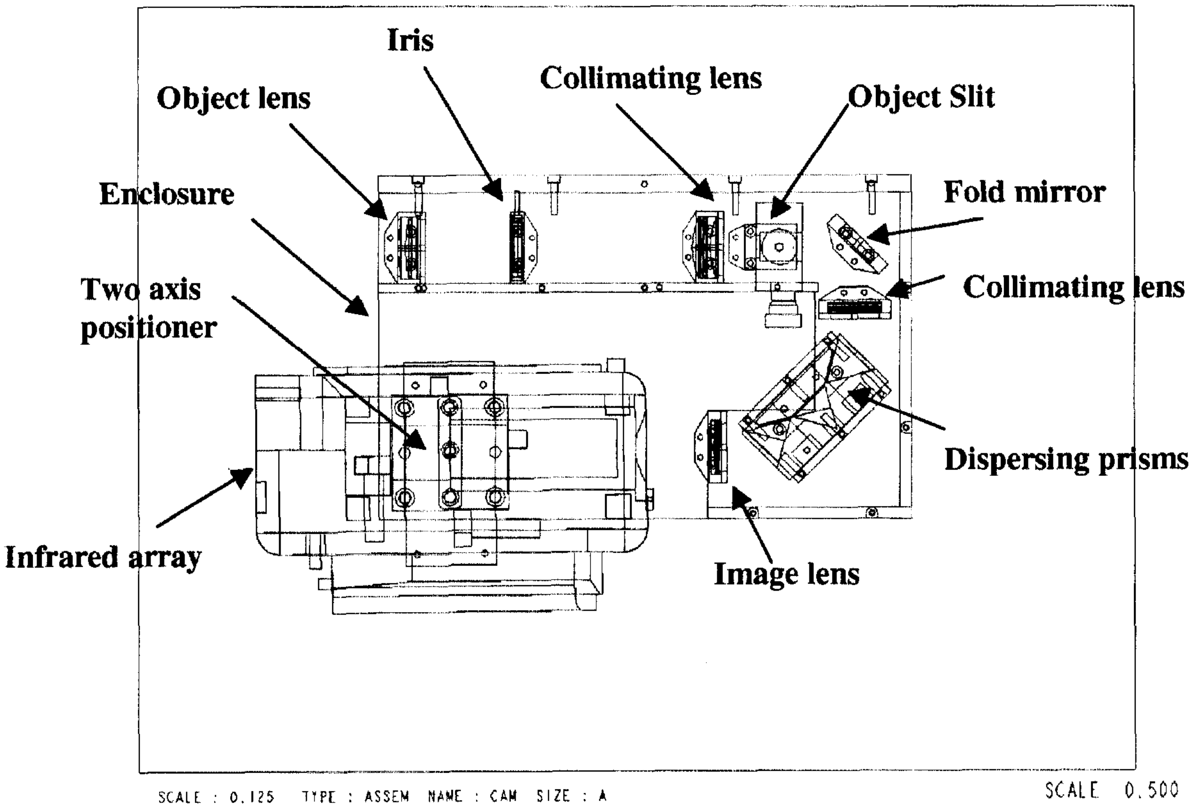

Figure 4. Schematic diagram of the 2-D imaging spectrometer.

from a fifty mm line source is imaged by an object lens and two collimating lenses to one side of the dispersing elements. The size of the source is controlled by an iris and a slit as shown in the Fig. 4. A fold mirror is used to reduce the size of the package. The line image is dispersed into the spectral components by three calcium fluoride prisms. The spectral image of the line source is imaged onto the infrared array detector using an imaging lens. The four lens assemblies are combination germanium-silicon achromats.

The array is a 324 x 244 element cooled PtSi array. The array is mounted on a two axis positioning stage to allow for alignment. All the other optical components have been machined to positional tolerances of 12 microns. Therefore, they are pinned down and do not have to be aligned. The two axis positioning stage is provided to allow for some tolerances in the machining of the lenses and slits.

The 2-D imaging spectrometer was fabricated by En'Urga Inc. Calibration and evaluation of the spectrometer was completed at Purdue University.

3.4 Evaluation of the Spectrometer

The objective of the present SBIR was to obtain the local intensities from the path integrated intensities, while accounting for self absorption. The path integrated intensities obtained at a height of 40 mm above the burner for a methane/air laminar diffusion flame is shown in Fig. 5. The methane/air diffusion flame was stabilized on a 12 mm diameter burner

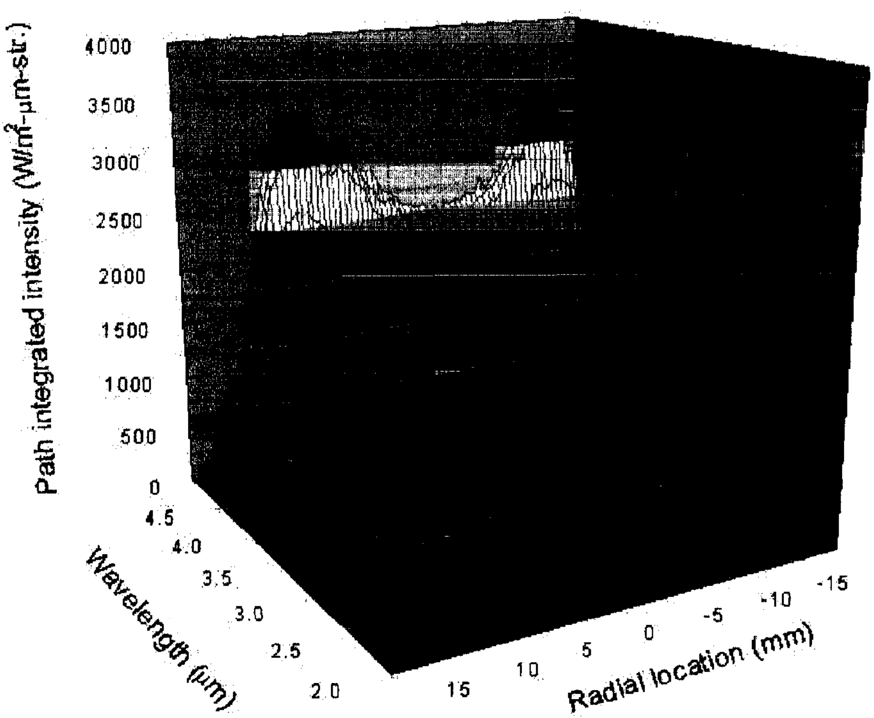

Figure 5. Path integrated intensities from a horizontal plane in a laminar flame.

with a co-flow of air. The radiation from carbon dioxide (4.4 μm), water vapor (2.7 μm) and methane (3.2 μm) are clearly visible in the path integrated intensities.

The deconvolution of path integrated intensities to obtain local intensities utilized a maximum likelihood estimation method (Vardi and Lee, 1993). The deconvolution is performed one wavelength at a time. The maximum likelihood solution is obtained iteratively, and the iterative algorithm for any wavelength λ is briefly discussed below.

The geometry that was used to develop the method is shown in Fig. 6. Three of the

$\Delta S^1{}_1$ $\Delta S^2{}_2$

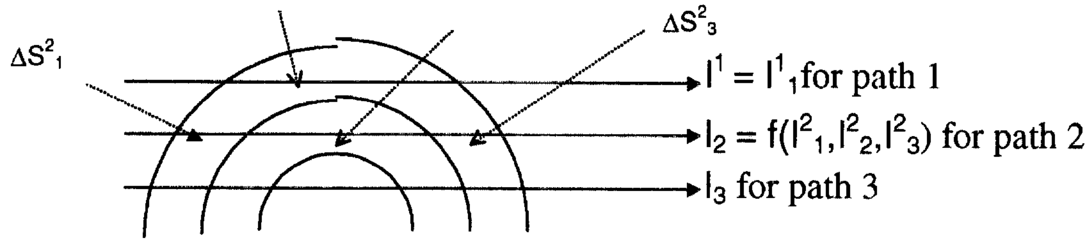

Figure 6. Schematic diagram of parallel paths in an axisymmetric flow.

outermost parallel paths through a laminar flame are shown in Fig. 6. The outermost path has one homogeneous segment (1) of length ΔS^1_1. The emission intensity of the homogeneous segment is I_1^1, and its transmittance is τ^1_1. The path integrated emission intensity of the path I^1 is equal to I^1_1. The superscript denotes the path index and the subscript denotes the segment index. The second path has three homogeneous segments of lengths ΔS^2_1, ΔS^2_2, and ΔS^2_3, with segment emission intensities of I^2_1, I^2_2 and I^2_3 and transmittance of τ^2_1, τ^2_2, and τ^2_3. For any path with index N, there are 2N+1 homogeneous segments associated with it.

The path integrated emission intensity I_N can be calculated from the emission intensities and transmittances of of the homogeneous segments as:

$$I_N = \sum_{i=1}^{2N+1} (I_i^N * \prod_{j=i+1}^{2N+1} \tau_j^N) \tag{1}$$

The deconvolution is an iterative algorithm based on the maximum likelihood estimation method of Vardi and Lee (1993). First, guessed values of local emission intensities are used in a forward convolution (using Eq. 1) with the transmittances of the homogeneous segments set at 1. During the forward convolution, the following relationships between the emission intensities and transmittances of the homogeneous segments amongst neighboring paths have to be maintained for axisymmetry.

$$I_i^N = (I_i^{N-1})^{(\Delta S_i^N / \Delta S_i^{N-1})} = I_{N+i}^N \tag{2}$$

$$\tau_i^N = (\tau_i^{N-1})^{(\Delta S_i^N / \Delta S_i^{N-1})} = \tau_{N+i}^N \tag{3}$$

Let the total number of path integrated measurements obtained be M. Then, using Eq. (1) with the guessed values of intensities (transmittance set to 1), we obtain M solutions for the path integrated intensities which in general are different from the measurements. It is noted that with the use of Eq. (2), only M values of intensities, corresponding to the centermost of the homogenous segments (I_i^1) for each path has to be guessed. The guessed values are then updated as follows:

$$\overset{k}{(X_i^i)} = \sum_{i=1}^{M} \sum_{j=1}^{M} \overset{k-1}{(X_i^i)} (\Im_{ij}/T_j)(I^i/X^i) \tag{4}$$

where X_i^i is the guessed values for the intensities of the middle segment of each of the M paths, and k is the iteration number. X^i is the path integrated intensity of the i^{th} path obtained from the forward convolution (Eq. 1), and I^i is the measured value of the path integrated intensity.

$\Im_{ij}$ is the is the contribution of the intensity from the j^{th} homogeneous segment to the path integrated intensity of path i. For each of the M path, there are two homogeneous segments with identical emission intensities, $\Im_{ij}$ can be obtained as:

$$\Im_{ij} = X_j^i \prod_{p=j+1}^{2i+1} \tau_p^i + X_{j+i}^i \prod_{p=j+i+1}^{2i+1} \tau_p^i \tag{5}$$

and T_J is the sum of the contributions from each segment to the M path integrated intensities and can be obtained as:

$$T_j = \sum_{i=1}^{M} \Im_{ij} \tag{6}$$

The value of X_i, $\Im_{ij}$ and T_j are calculated during the forward convolution and used in Eq. (4) to obtain an updated guess for the emission intensities X_i^i. The algorithm is very efficient and convergence is usually obtained in approximately 20 iterations. The iterations are terminated when the L2 norm of the difference between the measured intensities and calculated intensities defined as:

$$L2 = \left(\sum_{i=1}^{M} (X^i - I^i)^2 \right)^{1/2} \tag{7}$$

is less than 0.001.

The local emission intensities obtained from the measured path integrated intensities (see Fig. 6) are shown in Fig. 7. The local intensities show the CO_2, H_20 and CH_4 peaks very clearly. The CO_2 and H_2O peaks are at approximately the same location, while the CH_4 peak is closer to the center of the fire. This is expected since CH_4 is present only in the fuel rich regions of the fire.

During the first stage, the deconvolution algorithm neglected self absorption. The deconvoluted local intensities were then used to obtain spatially resolved temperatures, and

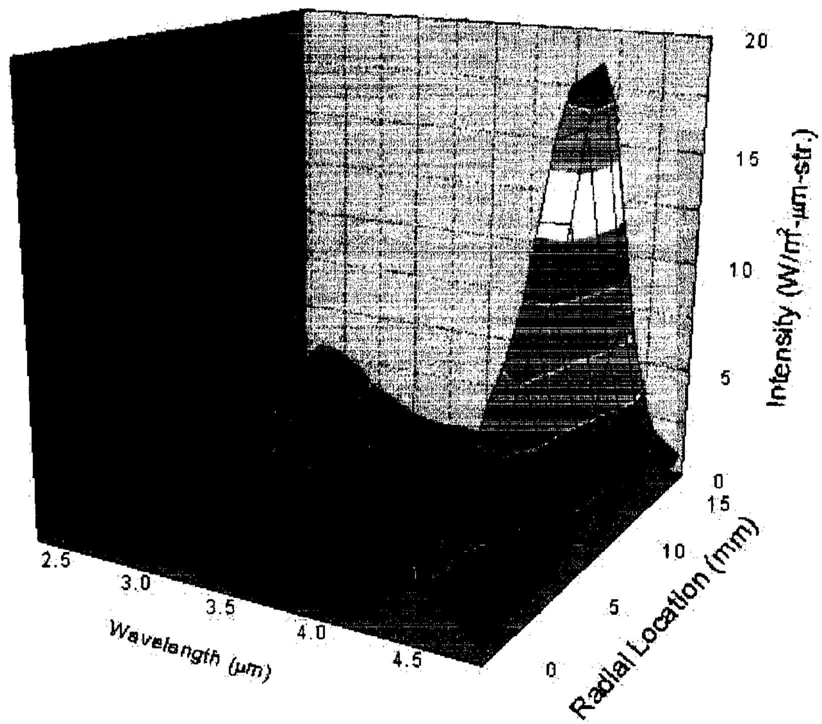

Figure 7. Local emission intensities obtained from the deconvolution algorithm.

gas species concentrations, using an iterative algorithm in conjunction with the RADCAL program. Once the local concentrations and temperatures were obtained, the local absorption coefficients were calculated. It was found that the path integrated transmittances in all cases were well above 0.9. Therefore, even addition of the local transmittances into Eq. (1) and (4) changed the local intensities by less than 5%. However, for an optically thick flame, it is necessary to introduce the local transmittances and recalculate local emission intensities till convergence is obtained (usually in four to five iterations).

The local gas concentrations and temperatures obtained from the converged local emission intensities, while accounting for self absorption, is shown in Fig. 8. The top panel shows the temperatures obtained from the local emission intensities. There is some noise in the data and a second-order curve fit is also shown as a solid line. The temperatures obtained are typical of a laminar diffusion flame. Thermocouple measurements were not available for direct comparison.

The bottom panel of Fig. 8 shows the major gas species (water vapor and carbon dioxide) concentrations obtained during the Phase II work and those obtained from the literature (Gore and Zhan, 1996). The gas chromatography measurements were obtained in a similar laminar diffusion flame at Purdue University. However, the co-flow was different for the flames. In addition, the calibration of the spatial co-ordinate with the aperture of the black body was accurate to only 20%. Therefore, the concentration profiles obtained with the IR emission spectroscopy is wider than those obtained using gas chromatography.

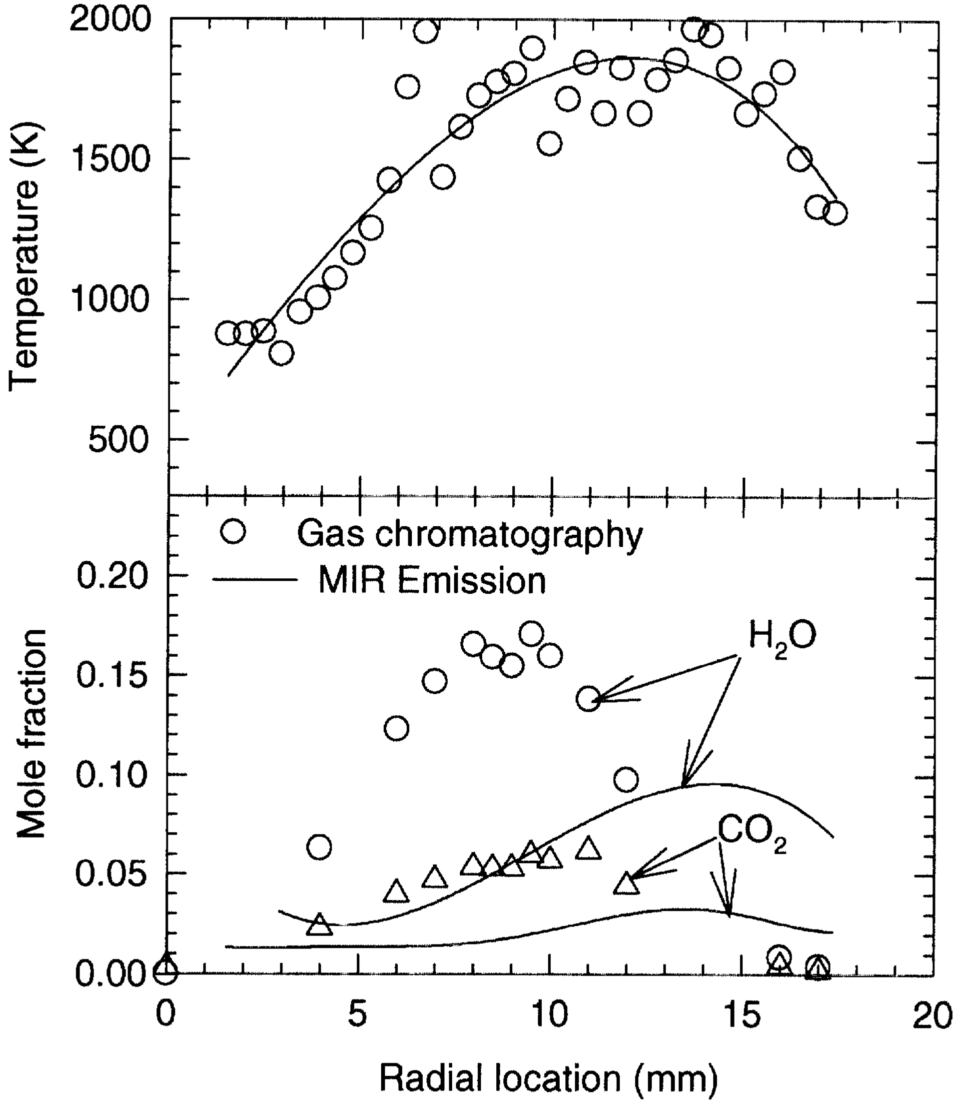

Figure 8. Local properties obtained from the deconvolution program.

The peak values of CO_2 and H_2O are also lower by a factor of 2. The are two possible reasons for this discrepancy. The imaging optics used in front of the camera provides a 10% curvature on the wavelength position (horizontal pixels). The spectral images obtained at Purdue neglected this curvature. Therefore, the spectra at 4.3 could be shifted by as much as 40 nm. This shift is sufficient to introduce a 50K variation in the temperatures obtained which will result in a 50% reduction of the concentrations. Current work is focussed on accounting for the wavelength curvature by calibrating the wavelength seen by each pixel using narrow band filters.

The second reason for the difference could be insufficient spectral resolution of the imaging spectrometer at 4.5 microns. The current procedure assumes that each pixel received monochromatic radiation. However, it is possible that there is a width to the wavelengths seen by each pixel. This will become evident when the wavelength calibration with the narrow band filters are carried out.

The CH_4 and CO concentrations obtained are shown in Fig. 9. Similar to the CO_2

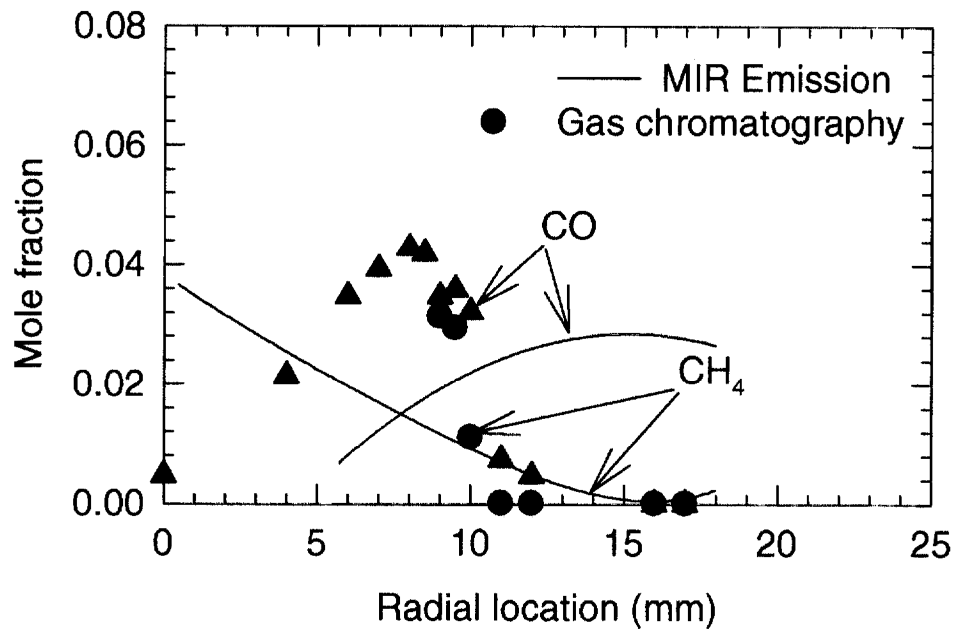

Figure 9. Local properties obtained from the deconvolution program.

and H_2O concentrations, the CO concentrations estimated by IR emission spectroscopy are a factor of two lower than that obtained using gas chromatography. This is consistent with the observation that temperatures are overestimate.

It is much more difficult to compare the two techniques for CH_4 since the lower limit of emission spectroscopy is approximately 1000 K, and CH_4 is present even at 300 K since it is a fuel. The results are shown in Fig. 9 purely just for completeness. It is not anticipated that IR emission spectroscopy will provide accurate results for the fuel.

The correct spectral location and widths seen by each pixel will be obtained during experiments at NIST. The wavelength calibration will then be used to resolve the concentration differences between the previous gas chromatography measurements and the current IR emission intensity measurements.

3.5 Phase II: Results and Conclusions

The following results and conclusions can be drawn from the Phase II SBIR work.

(1) An algorithm for determining inlet temperatures in natural gas turbine engines from four wavelength infrared intensity measurements was successfully developed and evaluated.

(2) A study of the different methods of obtaining four wavelength infrared intensity measurements for the development of a gas turbine temperature sensor was completed.

(3) A 2-D infrared imaging spectrometer was designed and fabricated.

(4) A deconvolution algorithm to provide local emission intensities from integrated measurements in laminar flames was developed and evaluated using synthetic and experimental data.

(5) The deconvolution algorithm provided very accurate local intensities from the synthetic data.

(6) Initial evaluation of the spectrometer and the deconvolution algorithm at Purdue University was completed. The results provided reasonable temperature measurements, but the gas concentrations obtained were much lower than those obtained using gas chromatography. The reason for the discrepancy is the lack of accurate calibration for the spectral location and width.

(7) Reliable calibration of the spectral location and width using narrow band filters is essential for accurate determination of gas concentrations.

(8) The 2-D imaging spectrometer was delivered to the National Institute of Standards and Technology.

4. Phase III commercialization

A part of the Phase II work has resulted in the development of a gas temperature sensor for use with commercial natural gas turbine engines. The sensor has been licensed for manufacturing and marketing to AMETEK Aerospace Products Inc. The prototype sensors will be installed and tested at Solar Turbines Inc. by the end of 1999.

A new company called Spectraline Inc. has been started by En'Urga Inc. The prototype 2-D array developed during the Phase II SBIR has been commercially made available under the Spectraline label. The Spectraline label was trademarked in July 1999. Venture capital for marketing the 2D spectrometer has been requested from outside financial sources.

5. References

Best, P. E., Chien, P. L., Carangelo, R. M., Solomon, P. O., Danchak, M., and Ilovici, I., Combust. Flame, vol. 85, p. 309 (1991).

Bishop, Y. M. M., Fienber, S. E., and Holland, P. W., Discrete Multivariate Analysis: Theory and Practice, MIT Press, Cambridge (1975).

Chen, F. P., and Goulard, R., JQSRT, vol. 16, pp. 819-827 (1976).

Choi, M. Y., Hamins, A., Mullholland, G. W., and Kashiwagi, T., Combust. Flame, vol. 99, p. 174 (1995).

Cover, T. M., IEEE Trans. Inform. Theory, vol. 30, pp. 369 (1984).

Crosley, D. R. and Smith, G. P., Opt. Eng., vol. 22, p. 545 (1983).

Deans, S. R., The Radon Transform and Some of its Applications, Wiley, New York (1983).

Durao, D. F. G., Heitor, M. V., Whitelaw J. H., and Witze, P. O., Combustion Flow Diagnostics, Kluwer Academic Publishers, Netherlands (1992).

Eckbreth, A. C., Boncyzk, P. A., and Verdieck, J. F, Prog. Energy Combust. Sci., vol. 5, p. 253 (1979).

Grosshandler, W. L., Int. J. Heat Mass Trans., vol. 23, p. 1447 (1980).

Gore, J. P. and Zhan, N. J., Combust. Flame, vol. 105, p. 414 (1996).

Hanson, R. K., Varghese, P. L., Schoenung, S. N., and Falcone, F. K., Laser Probes for Combustion Chemistry, ACS-Symposium Series, vol. 134, p. 413 (1980).

Nyden, M. R., Vallikul, P., and Sivathanu, Y. R., JQSRT, vol. 55, pp. 345 (1996).

Ramachandran, G. N. and A. V. Lakshminarayanan, Proc. Nat. Acad. Sci., vol. 68, p. 2236, (1970).

Ravichandran, M., and Gouldin, F. C., Appl. Opt., vol. 27, p. 4084 (1988).

Santaro, R. J., Semerjian, H. G., Emmerman, P. J., and Goulard, R., Int. J. Heat Mass Transfer, vol. 24, p. 1139 (1981).

Shepp, L. A., and Logan, B. F., IEEE Trans. Nucl. Sci., vol. NS-21, p. 21 (1974).

Shepp, L. A. and Vardi, Y., IEEE Trans. Med. Imgng., vol. 1, p. 113 (1982).

Sivathanu, Y. R., Gore, J. P., and Dollinar, J., Combust. Sci. Tech., vol. 76, p. 45 (1991).

Sivathanu, Y. R. and Gore, J. P., Combust. Sci. Tech., vol. 80, p. 1 (1991).

Sivathanu, Y. R., and Faeth, G. M., Combust. Flame, vol. 89, p. 150 (1990).

Sivathanu, Y. R., Gore, J. P., and Dollinar, J., Combust. Sci. Tech., vol. 76, p. 45 (1991).

Sivathanu, Y. R., and Gore, J. P., JQSRT, vol. 50, pp. 483 (1993).

Sivathanu, Y. R., Hamins, A., Hagwood, C., and Kashiwagi, T., Proceedings of the Joint Technical Meeting of the Central and Western States Sections and the Mexican National Section of the International Combustion Institute and American Flame Research Committee, p. 92 (1995).

Sivathanu, Y. R., and Tseng, L. K., Fire Safety Journal, vol. 29, p. 301(1998).

Solomon, P. R., Philip, E. B., Carangelo, R. M., Markham, J. R., Chien, P. L., Santoro, R. J., and Semerjian, H. R., Twenty-First Symposium (International) on Combustion, The Combustion Institute, Pittsburgh, PA, p. 1763 (1986).

Tourin, R. H., Spectroscopic Gas Temperature Measurement, Elsevier, New York, NY (1983).

Uchimaya, H., Nakajima, M., and Yuta, S., Appl. Opt., vol. 24, p. 4111 (1985).

Vaidya, D. B., Horvath, J. J., and Green, A. E. S., Applied Optics, vol. 21, p. 3357 (1982).

Vardi, Y., and Lee, D., J. R. Statist. Soc. B, vol. 55, p. 569 (1993).

Zhu, Y.J., Sivathanu, Y. R., and Gore, J. P., Heat Transfer in Combustion and Fire, HTD-vol. 310, pp. 120-127, ASME, New York, NY (1997).

6. FINANCIAL REPORT

Cost Incurred from 3/20/99 to 7/20/99

PI (Dr. Yudaya Sivathanu)	400.00

Total Labor	400.00
Fringes (@ 12.5%)	50.00

Total labor + fringes	450.00
Partial cost of spectrometer and optics	9,665.04
Partial cost of Purdue subcontract	26,081.50

Subtotal of Labor and Direct costs	36,196.54
Administrative overhead (@ 10%)	3,619.65

Total expenses incurred	39,816.19
Fee (@ 7% minus cost sharing)	154.81

Total expenses for the current report period	**39,971.00**
	===========

Cost Incurred from 8/20/97 to 7/20/99

PI (Dr. Yudaya Sivathanu)	23,484.00
Design Engineer (Mr. Rony Joseph)	26,700.00
Programmer	1,773.20

	51,957.20
Fringes (@ 12.5%)	6,494.66

Total labor + fringes	58,451.86
Cost of camera and spectrometer optics	79,584.68
Purdue subcontract	34,000.00

Subtotal of Labor and Direct costs	172,036.54
Administrative overhead (@ 10%)	17,203.65

Total expenses incurred	189,240.19
Fee (@ 7%)	10,614.81

Total expenses from the start of the project	**199,855.00**
	===========

NIST-114 **U.S. DEPARTMENT OF COMMERCE**

(ERB USE ONLY)	
ERB CONTROL NUMBER	DIVISION
PUBLICATION REPORT NUMBER: NIST GCR 99-777	CATEGORY CODE
PUBLICATION DATE: September 1999	NUMBER PRINTED PAGES

INSTRUCTIONS: ATTACH ORIGINAL OF THIS FORM TO ONE (1) COPY OF MANUSCRIPT AND SEND TO

TITLE AND SUBTITLE (CITE IN FULL)

Rapid Scanning Infrared/Near Infrared Spectrometer

CONTRACT OR GRANT NUMBER

TYPE OF REPORT AND/OR PERIOD COVERED

AUTHOR(S) (LAST NAME, FIRST INITIAL, SECOND INITIAL)

Sivathanu, Y.
Joseph, R.
Lim, J., Zheng, Y., and Gore, J.

PERFORMING ORGANIZATION (CHECK (X) ONE BOX)

- [ ] NIST/GAITHERSBURG
- [ ] NIST/BOULDER
- [ ] JILA/BOULDER

LABORATORY AND DIVISION NAMES (FIRST NIST AUTHOR ONLY)

SPONSORING ORGANIZATION NAME AND COMPLETE ADDRESS (STREET, CITY, STATE, ZIP)

PROPOSED FOR NIST PUBLICATION

- [ ] JOURNAL OF RESEARCH (NIST JRES)
- [ ] J. PHYS. & CHEM. REF. DATA (JPCRD)
- [ ] HANDBOOK (NIST HB)
- [ ] SPECIAL PUBLICATION (NIST SP)
- [ ] TECHNICAL NOTE (NIST TN)
- [ ] MONOGRAPH (NIST MN)
- [ ] NATL. STD. REF. DATA SERIES (NIST NSRDS)
- [ ] FEDERAL INF. PROCESS. STDS. (NIST FIPS)
- [ ] LIST OF PUBLICATIONS (NIST LP)
- [ ] NIST INTERAGENCY/INTERNAL REPORT (NISTIR)
- [ ] LETTER CIRCULAR
- [ ] BUILDING SCIENCE SERIES
- [ ] PRODUCT STANDARDS
- [x] OTHER NIST GCR

PROPOSED FOR NON-NIST PUBLICATION (CITE FULLY) [ ] U.S. [ ] FOREIGN

PUBLISHING MEDIUM

- [x] PAPER
- [ ] CD-ROM
- [ ] DISKETTE (SPECIFY)
- [ ] OTHER (SPECIFY)

SUPPLEMENTARY NOTES

ABSTRACT (A 2000-CHARACTER OR LESS FACTUAL SUMMARY OF MOST SIGNIFICANT INFORMATION. IF DOCUMENT INCLUDES A SIGNIFICANT BIBLIOGRAPHY OR LITERATURE SURVEY, CITE IT HERE. SPELL OUT ACRONYMS ON FIRST REFERENCE.) (CONTINUE ON SEPARATE PAGE, IF NECESSARY.)

This Phase II SBIR project report covers the development of a 2-D imaging spectrometer for the determination of the local gas species concentrations and temperatures from a laminar flame, and its extension for commercial application as a gas temperature sensor.

Three separate tasks were undertaken during the Phase II work. The first task was the development of an optimized algorithm and hardware design to obtain gas temperatures from a high frequency multi-wavelength sensor. The second task was the development of an imaging spectrometer to obtain spectral radiation intensities along a horizontal plane from a laminar diffusion flame. The third task was the development of a deconvolution algorithm to obtain gas species concentrations and temperatures from the spectral radiation intensity measurements.

Based on the Phase II research, the following results were obtained. A robust algorithm for determining the gas temperatures at the inlet of a natural gas turbine engine, from measurements of infrared radiation intensities, was developed, evaluated and licensed for commercial production. A study of the different methods of obtaining infrared radiation intensities for a turbine-inlet gas temperature sensor was completed. A prototype 2-D infrared imaging spectrometer was designed, fabricated and delivered to the National Institute of Standards and Technology.

A deconvolution algorithm to obtain local radiation intensities from path integrated measurements was developed and evaluated. The 2-D imaging spectrometer was used to obtain spectrally and spatially resolved infrared radiation intensities in a laminar natural gas diffusion flame. A new company called Spectraline Inc. has started to market the 2-D imaging spectrometer.

KEY WORDS (MAXIMUM OF 9; 28 CHARACTERS AND SPACES EACH; SEPARATE WITH SEMICOLONS; ALPHABETIC ORDER; CAPITALIZE ONLY PROPER NAMES)

algorithms; fire research; gas temperature; image intensifiers; infrared spectrometer; laminar flames; measurements

AVAILABILITY

- [x] UNLIMITED
- [ ] FOR OFFICIAL DISTRIBUTION - DO NOT RELEASE TO NTIS
- [ ] ORDER FROM SUPERINTENDENT OF DOCUMENTS, U.S. GPO, WASHINGTON, DC 20402
- [x] ORDER FROM NTIS, SPRINGFIELD, VA 22161

NOTE TO AUTHOR(S): IF YOU DO NOT WISH THIS MANUSCRIPT ANNOUNCED BEFORE PUBLICATION, PLEASE CHECK HERE. [ ]